

Giant optical anisotropy in a single InAs quantum dot in a very dilute quantum-dot ensemble

I. Favero, G. Cassabois,* A. Jankovic, R. Ferreira, D.
Darson, C. Voisin, C. Delalande and Ph. Roussignol
*Laboratoire Pierre Aigrain, Ecole Normale Supérieure,
24 rue Lhomond 75231 Paris Cedex 5, France*

A. Badolato and P. M. Petroff
*Materials Department and Electrical and Computer Engineering Department,
University of California, Santa Barbara, California 93106, USA*

J. M. Gérard
*CEA-CNRS-UJF "Nanophysics and Semiconductors" Laboratory,
CEA/DRFMC/SP2M, 17 rue des Martyrs 38054 Grenoble Cedex 9, France*

(Dated: February 2, 2008)

Abstract

We present the experimental evidence of giant optical anisotropy in single InAs quantum dots. Polarization-resolved photoluminescence spectroscopy reveals a linear polarization ratio with huge fluctuations, from one quantum dot to another, in sign and in magnitude with absolute values up to 82%. Systematic measurements on hundreds of quantum dots coming from two different laboratories demonstrate that the giant optical anisotropy is an intrinsic feature of dilute quantum-dot arrays.

PACS numbers: 78.67.Hc, 78.55.Cr, 78.66.Fd

Semiconductor quantum dots (QDs) offer a huge potential for the development of nanodevices. Recent papers report breakthroughs where a single QD serves as the physical support for the realization of an all-optical quantum gate [1], a single-photon source [2] for indistinguishable photon generation [3], and an optically triggered single-electron source [4]. In some novel QD devices, the polarization of the QD optical response could play a central role on their characteristics. For example, the carrier quantum cascade in a QD has been proposed for the generation of polarization-entangled Bell states in quantum information processing [5]. In the field of spintronics, the conversion of photon polarization to electron spin has the potential to provide spin-polarized carriers [6].

Assuming rotational symmetry of the QD along the [001] growth axis, one predicts, for the fundamental interband transition, two bright electron-hole pair states which are degenerate and excited by orthogonal circularly polarized light states. However, different microscopic effects break the QD rotational invariance such as the atomistic asymmetry of the crystal [7], and the anisotropy of the QD shape or composition [7, 8]. Because of the electron-hole exchange interaction the new QD eigenstates correspond to two linearly polarized transitions, $|X\rangle$ and $|Y\rangle$, which are aligned along two orthogonal axes of the nanostructure. Theoretical calculations predict so far almost equal oscillator strengths for both transitions [7].

Polarized photoluminescence (PL) spectroscopy in strongly confined InAs QDs has been employed by various groups to study, in single QDs, the fine structure of the fundamental transition and the degree of linear/circular polarization of its emission [9, 10, 11, 12, 13]. Linearly polarized doublets are observed with an energy splitting ranging from a few tens of μeV [12, 13] to several hundreds of μeV [10, 11]. If the PL intensity of both linearly polarized transitions is added, a net linear optical anisotropy of a few percents is obtained (except for the value of thirty percents mentioned in Ref. [14]), in agreement with the available theoretical framework.

In this Letter, we present the experimental evidence of giant optical anisotropy in single InAs QDs. Polarization-resolved PL spectroscopy in single QDs reveals a linear polarization ratio which fluctuates, from one dot to another, in sign and in magnitude with absolute values up to 82%. We do not observe any dependence of the linear polarization on incident power, temperature and excitation laser polarization. We interpret the QD optical anisotropy as due to different oscillator strengths for the two linearly polarized states. Sys-

tematic measurements on hundreds of QDs coming from two different laboratories allow us to demonstrate that the giant optical anisotropy is an intrinsic feature of dilute QD arrays. On the contrary, the optical anisotropy is much smaller for QDs belonging to dense arrays.

Single-QD spectroscopy at low temperature is performed by standard micro-PL measurements in the far field using a microscope objective in a confocal geometry. The excitation beam is provided by a linearly polarized He:Ne laser. The signal is detected, after spectral filtering by a 32 cm monochromator, either by a LN₂-cooled charge-coupled-device (CCD) for high signal-to-noise measurements with a spectral resolution of 180 μeV , or by a low noise Si-based photon counting module for ultra-precise linewidth measurements using interferometric correlation with a sub- μeV spectral resolution [15]. Polarization-resolved experiments are implemented by using a rotating half-wave retarder and a fixed linear polarizer in front of the spectrometer in order to avoid detection artifacts due to the anisotropic response function of the setup. The analysis axes X and Y are orthogonal and the X axis is parallel either to the $[110]$ or to the $[1\bar{1}0]$ crystallographic direction of the sample.

We present experimental data obtained for samples containing a single layer of InAs QDs grown on standard (001) GaAs substrates. Unlike previous work devoted to the study of the average polarization of QD ensembles [16, 17], we explore here the PL polarization properties in *single* QDs in *dilute* and *dense* QD arrays. Our self-assembled QDs (base ~ 20 nm, height ~ 2 nm) are obtained by molecular beam epitaxy in the Stranski-Krastanow growth mode. The transition from layer-by-layer growth to three-dimensional islanding occurs for a critical thickness of 1.7 monolayer in InAs. Owing to a gradient of the InAs layer thickness in our samples, three different regions can be identified on the surface of the wafers [18]: region (I) in two-dimensional growth mode with no QDs, region (III) in three-dimensional growth mode with an areal QD density of $10^3 \mu\text{m}^{-2}$ and an intermediate region (II), the so-called border region at the onset of QD nucleation, corresponding to a very dilute QD ensemble. The QDs studied in this paper come from three distinct wafers labelled A , B and C , where we stress that C was grown in a different laboratory from A and B . In the following, we present measurements on a set of four samples: $A_{(II)}$ and $C_{(II)}$ corresponding to dilute QD arrays in the border region (II) of wafers A and C , and $B_{(III)}$ and $C_{(III)}$ corresponding to dense QD arrays in region (III) of wafers B and C . Let us finally note that mesa patterns [19] are processed in our four samples in order to perform polarization-resolved single QD spectroscopy in similar conditions, although the etching of

mesas is not necessary in $A_{(II)}$ and $C_{(II)}$ because of the low QD density.

We first present a striking experimental evidence of giant optical anisotropy obtained for a single QD in sample $A_{(II)}$, hereafter called QD1. A low-temperature PL spectrum recorded with the CCD is displayed in the inset of Fig. 1. We observe a resolution-limited sharp line corresponding to electron-hole recombination in the single QD. Rotation of the half-wave retarder produces a strong variation of the PL signal intensity which is maximum and minimum for the X and Y analysis axes, respectively. The ratio I_X/I_Y of the measured intensities is as high as 10 for this single QD, giving a linear polarization ratio $P_L=(I_X-I_Y)/(I_X+I_Y)$ of 0.82 ± 0.05 . Rotation of the excitation laser polarization does not induce any modification. Further inspection of the emission polarization with a quarter-wave retarder allows us to exclude the existence of two orthogonal elliptically polarized states. These observations are in agreement with the expected linearly polarized transitions in QDs of reduced symmetry. We are not able to resolve the fundamental transition doublet corresponding to the two different polarizations. The effective energy splitting resolution of our setup is roughly 45 μeV which gives us an upper bound for the splitting energy of the fundamental doublet.

We now discuss the variation of the linear polarization ratio with the experimental conditions. In Fig. 1 we display the different power-dependent measurements performed on QD1. The spectrally integrated intensity [Fig. 1(a)] shows a linear increase with the incident power, followed by the standard saturation behavior. Interferometric correlation measurements of the QD linewidth allow us to evidence that the QD line keeps a Lorentzian profile, and that its width, which is independent from the polarization analysis axis, increases by a factor 3 with incident power [Fig. 1(b)]. Such a phenomenology reveals environment effects on the QD optical properties, likely coming from Coulomb correlations between carriers in the QD and its environment [20]. When increasing the incident power, the linear polarization ratio remains fairly constant [Fig. 1(c)]. We can thus exclude any difference in the capture efficiency for the $|X\rangle$ and $|Y\rangle$ states since their populations become equal above saturation. Temperature-dependent measurements in QD1 (not shown here) indicate identical features as follows. The QD transition energy follows the InAs bandgap energy when increasing the temperature. The linewidth variation exhibits the usual thermo-activated broadening due to phonon dephasing [15] and the linewidth increases by a factor 16 between 10K and 70K. Nevertheless the linear polarization ratio is unchanged.

Since there is no dependence on incident power, temperature and excitation laser polar-

ization of the linear polarization ratio, we thus conclude that the optical anisotropy is not related to carrier relaxation nor to environment effects. This phenomenon, with the striking example of QD1 but also observed for all investigated QDs, appears to be intrinsically bound to the fine structure of the QD fundamental transition. In the picture of the linearly polarized doublet in a QD of reduced symmetry, we interpret the QD optical anisotropy as due to *different oscillator strengths* for the two linearly polarized states $|X\rangle$ and $|Y\rangle$.

To elucidate the condition for reaching, or reducing, the giant optical anisotropy, we have performed systematic measurements of the linear polarization ratio in roughly 400 QDs located in the four samples described above. Similarly to QD1, we always find the extrema of the PL signal intensity for the X and Y analysis axes and the exchange splitting energy is smaller than $45\text{ }\mu\text{eV}$. We want here to highlight the absence of correlation between the QD energy (ranging from 1.25 to 1.4 eV) and the linear polarization ratio of the PL emission. In Fig. 2 we display the histograms of the linear polarization ratio for samples $A_{(II)}$ (a), $B_{(III)}$ (b), $C_{(II)}$ (c), and $C_{(III)}$ (d). For each sample, the histogram is normalized to the number of investigated QDs so that we get the probability density of finding a given linear polarization ratio, in an interval of 0.05 width.

The average linear polarization ratio $\langle P_L \rangle$ ranges from $\langle P_L \rangle = -0.007$ in sample $C_{(III)}$ to -0.15 in sample $C_{(II)}$ with $\langle P_L \rangle = 0.12$ and -0.09 in samples $B_{(III)}$ and $A_{(II)}$, respectively. The small values of $\langle P_L \rangle$ show that QD ensembles exhibit a weak polarization anisotropy in our samples. Since there is no correlation between the QD energy and the linear polarization ratio, identical values are obtained by performing macroPL experiments in large mesas. These data are in agreement with previous studies reporting a moderate optical anisotropy in similar QD ensembles [16, 21].

With the single QD spectroscopy we gain new and useful information by resolving the statistical distribution of the linear polarization ratio. For samples $A_{(II)}$ and $B_{(III)}$ coming from the same laboratory, we observe a strong increase of the variance σ_{P_L} when passing from the dense QD array ($\sigma_{P_L} = 0.12$, Fig. 2(b)) to the dilute QD array ($\sigma_{P_L} = 0.38$, Fig. 2(a)). For samples $C_{(II)}$ and $C_{(III)}$ coming from wafer C grown in a *distinct* laboratory, we observe qualitatively the same behavior when passing from a dense region ($\sigma_{P_L} = 0.11$, Fig. 2(d)) to a dilute one ($\sigma_{P_L} = 0.2$, Fig. 2(c)). As a consequence, we see that the giant optical anisotropy is an intrinsic and universal characteristic of the intermediate region (II), the so-called border region at the onset of the Stranski-Krastanow growth mode where QD nucleation

is initiated. Despite the difference between samples grown in separate laboratories, we see, in the prospect of future studies in single QDs, that the border region can be exploited for studying the giant optical anisotropy in a single quantum dot. On the other hand, the possibility of restoring optical polarization isotropy is optimal in dense QD arrays.

Recent studies of dilute QD arrays by high resolution near-field imaging have revealed structural anisotropy as evidenced by QD nucleation at the upper-step edge of terraces [22]. Moreover, detailed AFM studies of the QDs nucleation and growth [23] show a strongly anisotropic shape of the QDs as it is covered by the capping GaAs. This shape anisotropy and elongation along the $[1\bar{1}0]$ axis is very pronounced in the low QD density region of the sample. A microscopic model taking into account the complex morphology and composition of the QDs from dilute arrays is to be developed in order to explain the very different oscillator strengths of the QD transitions as well as the sign of P_L . In fact, the linear polarization ratio P_L may be affected by the existence of an in-plane electric field, as discussed in a forthcoming publication.

In conclusion we present the experimental evidence of giant optical anisotropy in single InAs QDs which is attributed to a strong difference of the oscillator strengths of the two bright excitons. We show by systematic measurements that the giant optical anisotropy is an intrinsic feature of dilute QD ensembles.

M. Terrier and S. Olivier are gratefully acknowledged for their contributions to the processing of the mesa structures. LPA-ENS is "unité mixte (UMR 8551) de l'ENS, du CNRS, des Universités Paris 6 et 7". This work is financially supported by the region Ile de France through the project SESAME E-1751.

*Electronic address: Guillaume.Cassabois@lpa.ens.fr

-
- [1] X. Li, Y. Wu, D. Steel, D. Gammon, T. H. Stievater, D. S. Katzer, D. Park, C. Piermarocchi, and L. J. Sham, *Science* **301**, 809 (2003).
 - [2] P. Michler, A. Kiraz, C. Becher, W. V. Schoenfeld, P. M. Petroff, L. Zhang, E. Hu, A. Imamoglu, *Science* **290**, 2282 (2000).
 - [3] C. Santori, D. Fattal, J. Vuckovic, G. S. Solomon, and Y. Yamamoto, *Nature* **419**, 594 (2002).
 - [4] A. Zrenner, E. Beham, S. Stufler, F. Findeis, M. Bichler, and G. Abstreiter, *Nature* **418**, 612 (2002).
 - [5] O. Benson, C. Santori, M. Pelton, and Y. Yamamoto, *Phys. Rev. Lett.* **84**, 2513 (2000).
 - [6] C. E. Pryor and M. E. Flatté, *Phys. Rev. Lett.* **91**, 257901 (2003).
 - [7] G. Bester, S. Nair, and A. Zunger, *Phys. Rev. B* **67**, 161306 (2003).
 - [8] E. L. Ivchenko, *Phys. Status Solidi (a)* **164**, 487 (1997).
 - [9] Y. Toda, S. Shinomori, K. Suzuki, and Y. Arakawa, *Phys. Rev. B* **58**, 10147 (1998).
 - [10] M. Bayer, G. Ortner, O. Stern, A. Kuther, A. A. Gorbunov, A. Forchel, P. Hawrylak, S. Fafard, K. Hinzer, T. L. Reinecke, S. N. Walck, J. P. Reithmaier, F. Klopff, and F. Schäfer, *Phys. Rev. B* **65**, 195315 (2002), and references therein.
 - [11] J. J. Finley, D. J. Mowbray, M. S. Skolnick, A. D. Ashmore, C. Baker, A. F. G. Monte, and M. Hopkinson, *Phys. Rev. B* **66**, 153316 (2002).
 - [12] R. M. Stevenson, R. M. Thompson, A. J. Shields, I. Farrer, B. E. Kardynal, D. A. Ritchie, and M. Pepper, *Phys. Rev. B* **66**, 081302 (2002).
 - [13] B. Urbaszek, R. J. Warburton, K. Karrai, B. D. Gerardot, P. M. Petroff, and J. M. Garcia, *Phys. Rev. Lett.* **90**, 247403 (2003).
 - [14] C. Santori, D. Fattal, M. Pelton, G. S. Solomon, and Y. Yamamoto, *Phys. Rev. B* **66**, 045308 (2002).
 - [15] C. Kammerer, G. Cassaboies, C. Voisin, M. Perrin, C. Delalande, Ph. Roussignol, and J. M. Gérard, *Appl. Phys. Lett.* **81**, 2737 (2002).
 - [16] P. Yu, W. Langbein, K. Leosson, J. M. Hvam, N. N. Ledentsov, D. Bimberg, V. M. Ustinov, A. Y. Egorov, A. E. Zhukov, A. F. Tsatsulnikov, and Y. G. Musikhin, *Phys. Rev. B* **60**, 16680 (1999).
 - [17] M. Henini, S. Sanguinetti, S. C. Fortina, E. Grilli, M. Guzzi, G. Panzarini, L. C. Andreani,

- M. D. Upward, P. Moriarty, P. H. Beton, and L. Eaves, Phys. Rev. B **57**, 6815 (1998).
- [18] G. Cassaboïs, C. Kammerer, R. Sopracase, C. Voisin, C. Delalande, Ph. Roussignol, and J. M. Gérard, J. Appl. Phys. **91**, 5489 (2002).
- [19] J. Y. Marzin, J. M. Gérard, A. Izraël, D. Barrier, and G. Bastard, Phys. Rev. Lett. **73**, 716 (1994).
- [20] A. V. Uskov, I. Magnusdottir, B. Tromborg, and J. Mørk, and R. Lang, Appl. Phys. Lett. **79**, 1679 (2001).
- [21] S. Cortez, O. Krebs, P. Voisin, and J. M. Gérard, Phys. Rev. B **63**, 233306 (2001).
- [22] F. Patella, S. Nufri, F. Arciprete, M. Fanfoni, E. Placidi, A. Sgarlata, and A. Balzarotti, Phys. Rev. B **67**, 205308 (2003).
- [23] B. D. Gerardot, I. Shtrichman, D. Hebert, P. M. Petroff, J. Cryst. Growth, **252**, 44 (2003).

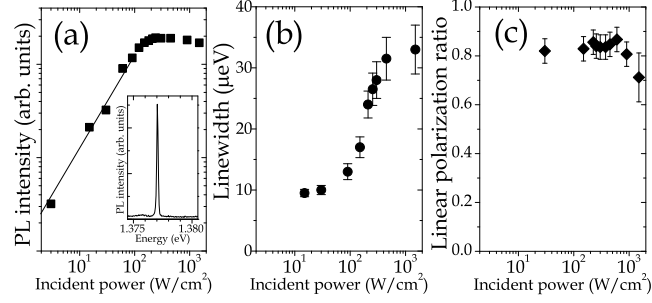


FIG. 1: Photoluminescence spectroscopy versus incident power for QD1 at 10K. (a) Spectrally integrated photoluminescence intensity, (b) linewidth (c) linear polarization ratio. (Inset): photoluminescence spectrum with an incident power of 30 W/cm².

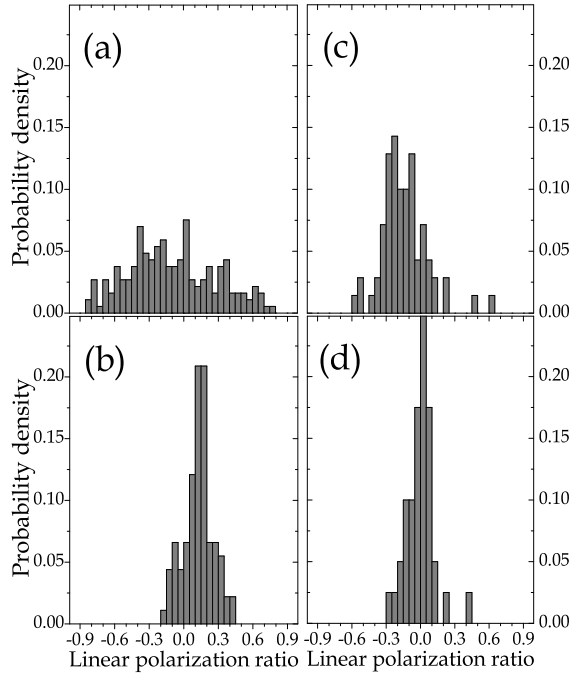


FIG. 2: Probability density of the linear polarization ratio in single QDs. Dilute QD arrays : samples $A_{(II)}$ (a) and $C_{(II)}$ (c). Dense QD arrays : samples $B_{(III)}$ (b) and $C_{(III)}$ (d). C was grown in a different laboratory from A and B .